



Corrosion Inhibition of Mild Steel in Hydrochloric Acid Solution using Methanolic Extracts of *Elsholtzia communis* and *Spilanthes acmella* as Green Inhibitors

JAY PRAKASH RAJAN^{ID}

Department of Chemistry, Pachhunga University College, Mizoram University, Aizawl-796001, India

Corresponding author: E-mail: jaypr33@gmail.com

Received: 23 June 2024;

Accepted: 31 July 2024;

Published online: 30 August 2024;

AJC-21739

The corrosion inhibition effect of methanolic extract of *Elsholtzia communis* inflorescence (ECI) and *Spilanthes acmella* (SA) towards the corrosion of mild steel in 1 N HCl solution was examined by means of weight loss, potentiodynamic polarization and electrochemical impedance spectroscopy (EIS) techniques. The corrosion rate was found to decrease with increasing ECI and SA concentration up to 0.5 g/L at 27 °C. The temperature effect on inhibition effect of plant extracts has also been discussed. Nyquist plots showed that methanolic extract of ECI yielded the best inhibition efficiency. The adsorption of inhibitor on the mild steel surface was found to obey the Langmuir adsorption isotherm through which various thermodynamic parameters were calculated and discussed. Surface morphology of the mild steel after exposing to test solutions in absence and presence of inhibitor were investigated by scanning electron microscope (SEM), which show that the corrosion of mild steel is retarded to great extent by ECI and SA extracts. The phytochemicals screening were performed by gas chromatography-mass spectroscopy (GC-MS) study based on this study effective inhibitor molecules and inhibitive mechanism can be established. The GC-MS and FT-IR studies of ECI and SA extracts indicated that the adsorption centre in green inhibitor probably due to presence of β -retinoid and its derivatives in ECI and SA extracts showed that the adsorption centre due to presence of fatty acid derivatives.

Keywords: Plant extracts, Mild steel, Phytochemicals, Aggressive medium, Inhibition efficiency.

INTRODUCTION

Mild steel is one of the most important basic materials with excellent structural and mechanical strength and hence extensively used in industry and engineering material, however; it tends to interact with environment and become corrode [1]. Acidic solution, especially hydrochloric acid is used in industry for various metallurgical processes and in petrochemical industry for alkylation and polymerization process. Aqueous acidic solution is highly corrosive and so carbon steel dissolves in such environment. The use of an inhibitor is the best method to inhibit the metal against corrosion in an aggressive medium [2]. Many synthetic organic compounds containing heterocyclic atoms (N, O, S), aromatic rings or π -bonds have been reported as effective acid corrosion inhibitors [2-5]. However, many of these synthetic compounds are toxic to human beings and environment as well. Hence, the use of natural products especially plant extracts containing wide range of organic compounds as corrosion inhibitor is the most practical and efficient for this purpose [6,7].

In recent years, plant extracts have been widely reported as acid corrosion inhibitor of steel in different acidic solutions [1,8]. Plant extracts are better choice as they possess large number of phytochemicals, show high inhibition efficiency at very low concentration in different aggressive medium and also environmental friendly. The most of the natural products are biocompatible, low toxic and provide alternatives to hazardous chemicals. The inhibitive action of natural products derived from plant materials is related to the presence of one or more heteroatoms (*viz.* oxygen, nitrogen, sulphur), aromatic rings or long alkyl chains [8]. Further, the exposed surface area of mild steel, molecular weight and structure of phytochemicals also affect their inhibition efficiency.

Recently, different parts (roots, seed, flowers, inflorescence, leaves) of various plants like *Opuntia*, *Aloe vera*, orange, mango, tobacco, black pepper, acacia gum have been reported as good inhibitors for steel in different acidic medium [9,10]. The interest is motivated by their extraordinary corrosion inhibition properties. These phytochemicals are excellent biocompatibility and it has been widely used as a functional material in the

development of corrosion inhibitors. Plant materials were selected based on the reported content of medicinal relevance and their common use. Beneficial effects of phytochemicals obtained from herbs and spices can be used into medicine as well as used for preventing of materials to degradation. In this context, uses of *Elsholtzia communis* inflorescence (ECI) and *Spilanthes acmella* (SA) herbs as medicine as well as vegetable in Mizo communities in Mizoram. *Spilanthes acmella* (SA) is a perennial flowering herb with a distinct odour and pungent flavour due to amides as their active ingredient, which can be a key component of a special ingredient in the spice. It is a useful as an anaesthetic, antifungal, antiseptic, anti-inflammatory and to treat several others chronic disorders [11].

The leaves and inflorescence of *Elsholtzia communis* inflorescence (ECI) are also used as flavouring agent in food as well as medicinal purpose [12]. The flavour and therapeutic ability of ECI is attributable to the presence of active phytochemical constituents such compounds as carotenoids derivative, terpenoids and phytosterol. It is worth to mention here that the ECI and SA are chosen for the present study because these are readily available, relatively cheaper and non-poison. To the best of our knowledge, these compounds have not been tested as corrosion inhibitors in previous work.

The present study consists of phytochemical screening of *Elsholtzia communis* inflorescence (ECI) and *Spilanthes acmella* (SA) methanol extracts and their corrosion inhibition effect using gravimetric and electrochemical techniques in 1 N HCl at 27 °C. The corrosion inhibition action of ECI and SA extracts are usually attributed to their adsorptive interaction with the mild steel surface. The stability of these phytochemical molecules on the mild steel surface depended on their structure, which has been established by Fourier transform infrared spectroscopy study. The surface of mild steel in absence and presence of inhibitors has also been characterized by SEM study.

EXPERIMENTAL

Inhibitor: Inflorescences of *Elsholtzia communis* and whole *Spilanthes acmella* plants were purchased from local markets of Aizawl, India. The collected plants were cleaned and shade dried at room temperature for 10 days, ground to fine powder using a mechanical grinder and 50 g of dust powder soaked in 500 mL of 60% methanol for 24 h at room temperature. The extract was filtered using Whatman No.1 filter paper. The filtrate was collected and the residue was re-extracted to get maximum extract of constituents. Solvent was removed by rotary evaporator using under reduced pressure at 40 °C.

Material preparation: Mild steel coupons of composition: 0.09 wt.% (C), 0.51 wt.% (Mn), 1.5 wt.% (Cr), 0.0219 wt.% (Si), 0.012 wt.% (P); 0.009 wt.% (Ni) and the remaining Fe were cut into rectangular form of dimension 2 cm × 2 cm × 0.5 cm abraded with different grades of emery paper up to 2000 grade to obtain well polished surface for gravimetric, electrochemical, FTIR and SEM studies. The same procedures and mild steel were used for different analytical measurements. The study was performed at different temperatures by using a water bath.

Gas chromatography-mass spectrometry analysis: The GC-MS of the crude methanolic extract of ECI and SA were performed using Autosystem XL gas chromatograph (Perkin-Elmer instrument, USA) equipped with Turbo Mass spectrophotometer (Perkin-Elmer instrument, USA) at Sophisticated Instrumentation Centre for Applied Research and Training (SICART) Vallabh Vidyanager, India. The GC-MS method using electron impact ionization technique with two fused silica capillary columns, 30 m × 0.25 mm ID, coated with D-I, 0.25 µm film. Helium was used as a carrier gas at constant pressure of 100 kPa. Injection port temperature; 523 K; flow rate 20mL/min. Temperature programme: 70-250 °C at the increasing rate of 10 °C/min, 70 °C and holding for 5 min and raised with 10 °C/min up to 250 °C and was hold for 15 min. The chromatographic data were processed with the mass detector operated with electron impact ionization (EI) mode with ionization energy 70 eV. Samples dissolved in methanol and were run fully in the range of 60-750 amu and the injection volume was 1 µL. The obtained mass spectra of plant extract were measured by Automated Mass Spectral Deconvolution and Identification System (AMDIS) and transferred to the National Institute of Standards and Technology (NIST) Mass Spectral library Search Program.

Gravimetric measurements: Corrosion rate and the inhibition efficiency of methanolic extracts of ECI and SA were estimated by weight loss method. A gravimetric measurement were conducted by suspending the mechanically polished pre-weighed mild steel of the same dimension as mentioned above in 100 mL of corrosive solutions for 3 h with and without addition of different concentrations of methanolic extracts of ECI and SA (0.1, 0.3 and 0.5 g/L) at 27 °C. Then the corrode specimens were washed with water and acetone, dried and reweighed.

Electrochemical measurements: The electrochemical measurements were performed using AUTOLAB (PGSTATE 12/20/302; Netherland) potentiostat instrument with GPES software assembled with three electrodes at 27 °C. A mild steel with an exposed area of 0.75 cm² was used as working electrode. Graphite rod and Ag/AgCl electrode with Luggin capillary were used as counter and reference electrodes, respectively. Prior to measurements of polarization curves and electrochemical impedance spectroscopy (EIS), the mild steel was mechanically abraded with emery papers from 80 grit to 2000 grit, respectively and then exposed to the corrosive medium at steady state open circuit potentials (OCP) for 3 h at 27 °C to attain equilibrium state. The polarisation resistant was measured for mild steel in 1 N HCl in absence and presence of different concentrations of ECI extract in the potential range from -0.650 V to 0.650 V versus OCP at a scan rate of 0.001 V/s.

Electrochemical impedance spectroscopy (EIS) studies carried out using a Gamry Instruments Reference 600 potentiostat/galvanostat/zero resistance ammeter (ZRA) on the same arrangement of electrode with freshly prepared working electrode. The impedance measurements were performed at open circuit potential (OCP) by the application of a periodic small amplitude (10 mV) ac voltage signal with a wide spectrum of frequency ranging from 100 kHz to 0.01 Hz. The impedance data were analyzed using Nyquist plots. In all measurements,

at least three similar results were considered and their average values have been reported.

Surface analysis: The methanolic extract of inflorescences of *Elsholtzia communis* and the material obtained by scratching off the mild steel after immersion in test solution for 3 h at 27 °C were dissolved in methanol, applied on glass plate and analyzed using a Perkin-Elmer System 2000 FTIR instrument from 4000 to 400 cm⁻¹.

The morphology of the mild steel was investigated before and after immersion in 1 N HCl without and with 0.5 g/L of methanolic extract of ECI using A Carl Zeiss LEO SUPRA 50VP FE-SEM at an accelerating voltage of 15 keV. For this study, mild steel were carefully polished to as described above and immersed in 1 N HCl for 3 h. Then, the specimens were cleaned with distilled water, dried and used for surface analysis.

RESULTS AND DISCUSSION

Identification of phytochemicals using GC-MS:

Obtained extract was analyzed by GC-MS and the constituent phytochemicals were identified with the help of NIST library. The results of GC/MS were obtained by measuring the peak area using Turbo Mass software and match with the hit list spectra of NIST library. Further, in view of corrosion inhibition study, structures of few organic molecules are presented in Table-1. The major phytochemicals present in methanolic extract of ECI are β-carotene, retinoic acid and retinol acetate as carotenoids derivatives. A combined GC-MS spectral data analysis revealed that the phytochemical constituents of ECI extract have potential to inhibit the acid corrosion of mild steel due to

presence of hetero atoms and π-bonds [9]. The whole plants of *Spilanthes acmella* (SA) contain various chemical constituents but unsaturated fatty acids are most interesting biologically active constituents. The major active constituents present in SA extracts are also given in Table-1 and these active constituents contain π-bonds and oxygen atoms.

Weight loss measurements: The variation of corrosion rate (C_{rate}) and inhibition efficiency (%IE) as functions of inhibitor concentration in acid media in absence and presence of methanolic extract of ECI and SA were calculated by standard method [9,10]. The C_{rate} and %IE were calculated by using the following equations [9]:

$$C_{rate} \left(\frac{\text{mg}}{\text{cm}^2 \times \text{h}} \right) = \frac{\Delta W}{AT} \quad (1)$$

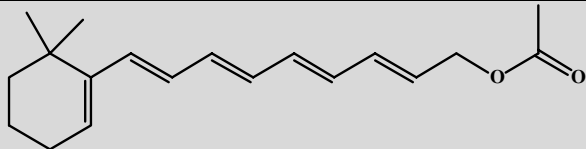
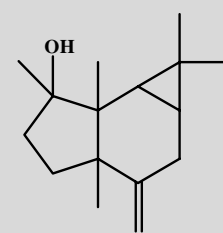
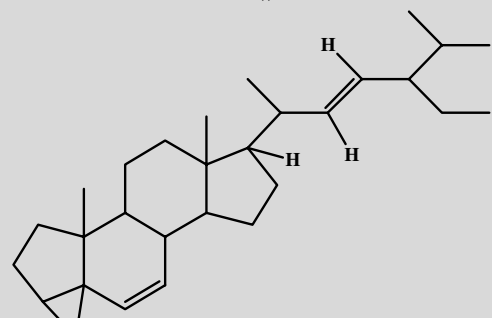
$$\%IE = \frac{C_{rate(\text{blank})} - C_{rate(\text{inh})}}{C_{rate(\text{blank})}} \times 100 \quad (2)$$

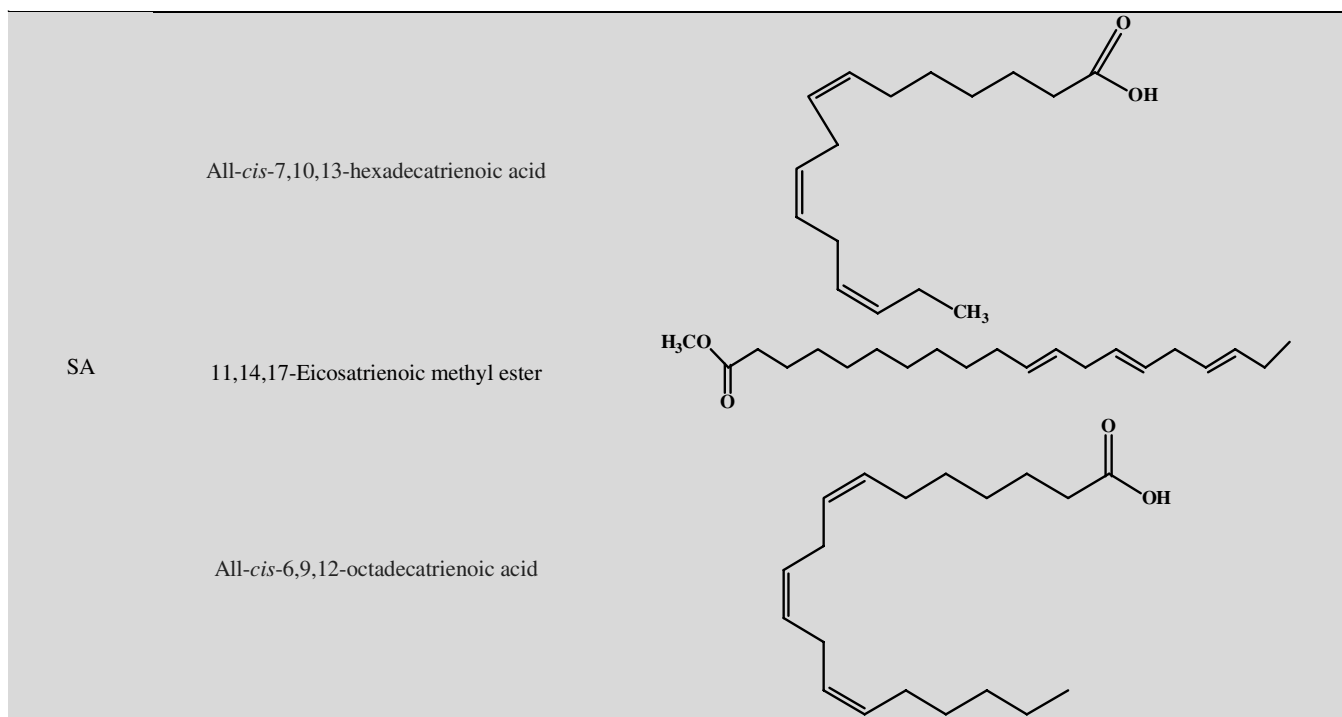
where ΔW is average weight loss in mg, A is total area of mild steel in cm², T is the exposure time (3 h). In eqn. 2, $C_{rate(\text{blank})}$ and $C_{rate(\text{inh})}$ are the corrosion rates on mild steel without and with different concentrations of inhibitor, respectively. The surface area covered by the inhibitor molecules on the mild steel, θ is given as:

$$\theta = \frac{(\%IE)}{100} \quad (3)$$

The obtained results of C_{rate} and %IE are shown in Table-2, which show that C_{rate} decreases with increasing in both ECI and SA extracts, whereas the value of %IE and θ increases with

TABLE-1
MAJOR PHYTOCHEMICAL CONSTITUENTS PRESENT IN METHANOLIC EXTRACT OF *Elsholtzia communis* INFLORESCENCE (ECI) AND *Spilanthes acmella* (SA) OBTAINED BY GC-MS ANALYSIS

Inhibitor	Major constituents	Molecular structure
ECI	β-Carotene	
	(-)-Spathulenol	
	6,22-Dien, 3,5-Dedihydro-stigmastan	



inhibitor concentration. The inhibition action is due to increase in extent of adsorption of inhibitor on the mild steel surface in 1 N HCl medium. In general %IE increases with the inhibitor concentration, but in acidic media, corrosion of metal is accompanied with evolution of H₂ gas, rise in temperature accelerates corrosion rates which results in a higher dissolution rate of metal.

TABLE-2
GRAVIMETRIC ANALYSIS FOR MILD STEEL IN 1 N HCl
AT 27 °C IN ABSENCE AND PRESENCE OF VARIOUS
CONCENTRATIONS OF ECI AND SA EXTRACTS

Inhibitor	Conc. (g/L)	C _{rate} (mg cm ⁻² h ⁻¹)	%IE	θ
ECI	Blank	5.87	00	0.00
	0.1	3.17	45	0.45
	0.3	1.11	81	0.81
	0.5	0.51	91	0.91
SA	Blank	4.36	00	0.00
	0.1	2.33	46	0.46
	0.3	0.88	79	0.79
	0.5	0.41	90	0.90

It has been observed from that %IE decreased with increase in temperature up to 67 °C. The decrease in %IE and increase corrosion rate with temperature might be attributed to desorption of the inhibitor molecule and increase exposure area of metal surface in acidic medium. The decreased in the adsorption at higher temperature indicated that physical adsorption of inhibitor.

Potentiodynamic polarization measurements: The cathodic and anodic current–potential measurements for mild steel in absence and presence of various concentrations of ECI and SA extracts in 1 N HCl solutions at 27 °C were derived by Tafel polarization method as shown in Fig. 1. The electro-

chemical parameters such as corrosion current density (I_{corr}), corrosion potential (E_{corr}) and cathodic and anodic Tafel slopes (β_a and β_c) were obtained by extrapolation of the linear segments of the cathodic and anodic curves as given in Fig. 1.

The obtained results from the potentiodynamic polarization experiments along with C_{rate} and %IE are listed in Table-3. It can be seen from Fig. 1 that at a given temperature, the cathodic curves are shifted towards lower cathodic curves with increasing concentration of both ECI and SA extracts in 1 N HCl. It also observed that the cathodic branch of polarization curves was rise parallel with increasing inhibitor concentration, it means that the inhibitor does not change the mechanism of hydrogen evolution. This could be attributed to the inhibitor molecules take place on the metal surface through a charge transfer mechanism. Thus, an addition of this inhibitor molecule suppresses the cathodic process and reduces the metal dissolution in acidic solution [13,14]. The β_c value were shifted toward more negative E_{corr} value, whereas the anodic one is slightly shifted toward lower E_{corr} . This indicated that the both extract influenced the cathodic reaction more than anodic reaction and hence the addition of these extracts are considered as cathodic inhibitors due to E_{corr} shifting towards more extent negative with by adding them to 1 N HCl solution [15]. From the anodic parts of the curves, the anodic reaction of mild steel does not exhibit significant inhibitive effect on the anodic reaction. In fact, all these inhibitors exhibit stronger inhibitive effect on the cathodic reaction than on the anodic one.

Table-3 reveals that in the presence of ECI and SA extracts, the change in E_{corr} value slightly shifted towards the negative direction compared to the blank solution. The values of β_c are more affected as compare to the values of β_a indicating the studied inhibitors predominant with cathodic type inhibitors. It was observed that β_a and β_c values of the SA extract in acid

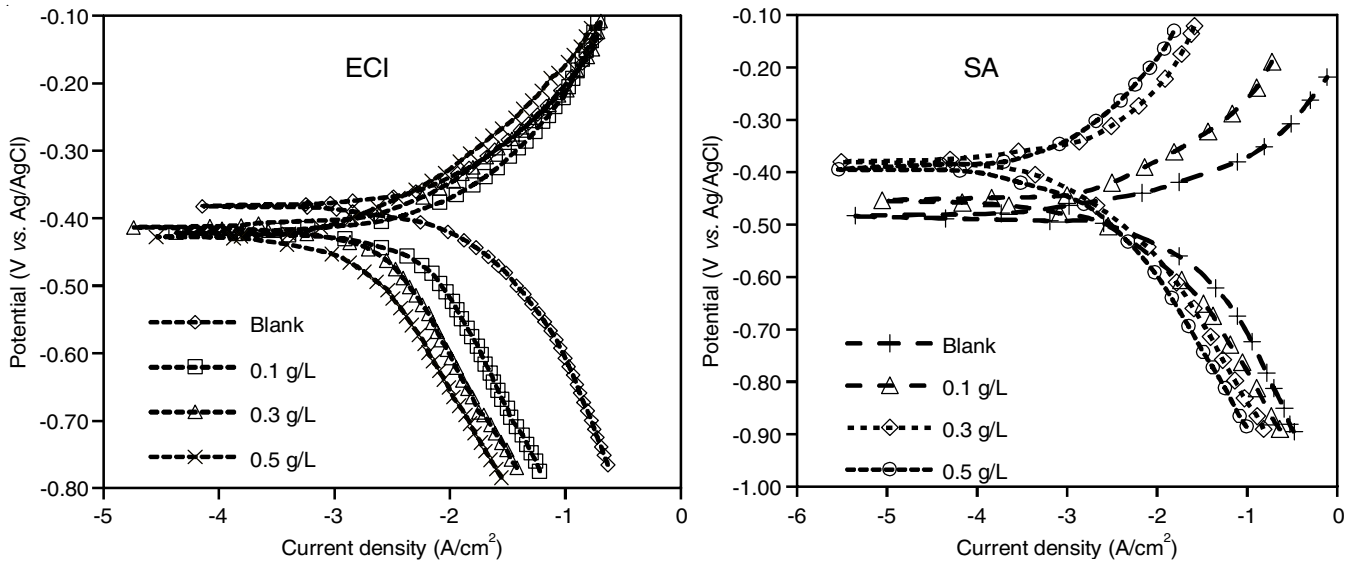


Fig. 1. Potentiodynamic polarization curves recorded for mild steel in 1 N HCl solution without and with different concentrations of ECI and SA at 27 °C

TABLE-3
TAFEL POLARIZATION PARAMETERS OBTAINED FOR MILD STEEL IN ABSENCE AND PRESENCE OF DIFFERENT CONCENTRATIONS OF ECI AND SA EXTRACT IN 1 N HCl AT 27 °C

Inhibitor	Conc. (g/L)	β_a (mV dec ⁻¹)	$-\beta_c$ (mV dec ⁻¹)	$-E_{\text{corr}}$ vs. Ag/AgCl (mV)	I_{corr} (mA cm ⁻²)	%IE
ECI	Blank	162	243	362	10.56	00
	0.1	176	334	431	5.97	43
	0.3	143	326	431	2.96	71
	0.5	129	279	428	1.03	90
SA	Blank	306	144	482	16.88	00.0
	0.1	284	131	425	5.44	67.7
	0.3	296	193	316	2.25	86.6
	0.5	299	182	337	1.44	91.4

solutions are smaller compared to that of the blank solution, but the displacement in E_{corr} is more than 85 mV with respect to E_{corr} of the blank, the inhibitor can be anodic type inhibitor.

The C_{rate} and θ of mild steel in 1 N HCl solutions without and with different concentrations of ECI and SA extracts were calculated by Tafel polarization data using following equations [15]:

$$C_{\text{rate}} (\text{mmpy}) = \frac{3.2 \times i_{\text{corr}} (\text{mA/cm}^2) \times \text{Eq. wt}}{D} \quad (4)$$

$$\theta = \frac{i_{\text{corr}(\text{blank})} - i_{\text{corr}(\text{inh})}}{i_{\text{corr}(\text{blank})}} \quad (5)$$

$$\%IE = \theta \times 100 \quad (6)$$

where C_{rate} is the corrosion rate in mmpy, i_{corr} is the corrosion current density in mA/cm²; Eq.wt is the equivalent weight of mild steel, molecular weight in mg/L of mild steel and D is the density.

It is evident from the data tabulated in Table-3 that the %IE observed at higher inhibitor concentration indicates that the adsorption process enhances with inhibitor concentration, which

increase the more inhibitor molecules are adsorbed on the metal surface, as results larger surface area coverage on metal surface. The results suggest the inhibitor molecules are adsorbed and decrease the intensity of corrosive attack with the addition of ECI and SA extracts by modifying the metal surface morphology [14].

Electrochemical impedance spectroscopy: Further, the electrochemical impedance spectroscopy (EIS) have been performed to confirm the adsorption of inhibitor molecules on the mild steel surface. This study provides the information regarding metal dissolution in corrosive medium through electrochemical characteristics such as double layer capacitance (C_{dl}), charge transfer resistance (R_{ct}) and solution resistance (R_s), which are extracted from intercept at the high frequency region (R_s) and the low frequency region (R_{ct}) intercept with the real axis. The impedance spectra were analyzed by fitting to the equivalent circuit model, which built by the Z-view software, based on the fitting for the steel-acid interface. The C_{dl} can be calculated by following equation:

$$C_{\text{dl}} = \frac{1}{2\pi R_{\text{ct}} f(-Z_{\text{max}})} \quad (7)$$

where f_{max} is the frequency of the imaginary part of impedance. Fig. 2 shows the Nyquist plots obtained by measuring the AC impedance for mild steel in 1 N HCl solution in the absence and presence of various concentration of ECI and SA extracts.

It is observed that a semicircular shape for impedance parameter in the blank and in the presence of various concentrations of ECI and SA extracts. This indicates that the inhibition mechanism does not depend on inhibitor concentration [8] and corrosion control process is charge transfer process [16]. Fig. 2 illustrates that the diameters of impedance plots increases with increasing concentration of ECI and SA extracts, which indicate that extent of adsorption of inhibitor molecules on the mild steel surface increases with inhibitor concentrations. The charge transfer resistance (R_{ct}) refers to restriction of electron transfer from the anode to the cathode, which as results in

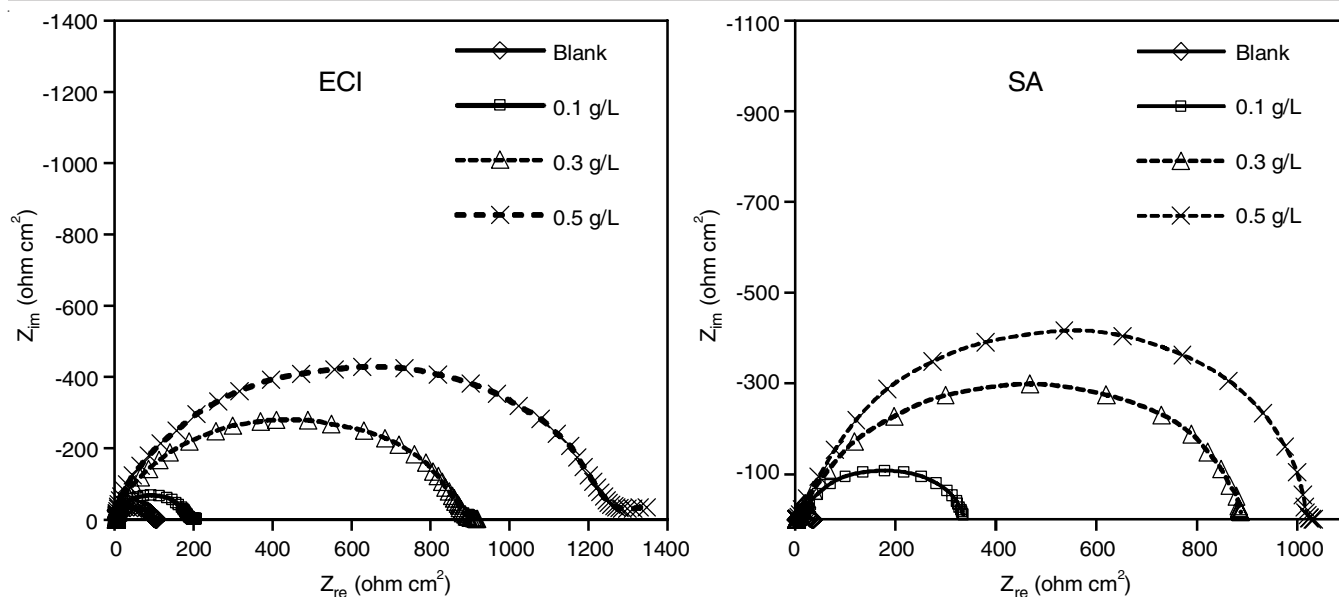


Fig. 2. Nyquist plots for mild steel in 1 N HCl solution without and with different concentrations of ECI and SA at 27 °C

oxidation of the metal in the acidic solution. This behaviour can be attributed to the plant extract adsorbed on metallic surface increases. The resistive and capacitive behaviour that was observed at mild steel test solution interface along with q and %IE are presented in Table-4. The EIS data presented in Table-4 clearly indicates that the values of C_{dl} decreases whereas the value of R_{ct} increases with inhibitor concentration as a result of that Nyquist plot of large diameter were observed in presence of green inhibitor.

TABLE-4
IMPEDANCE PARAMETERS FOR MILD STEEL IN
1 N HCl IN ABSENCE AND PRESENCE OF DIFFERENT
CONCENTRATIONS OF EXTRACT AT 27 °C

Inhibitor	Conc. (g/L)	R_s (Ω cm ²)	R_{ct} (Ω cm ²)	C_{dl} (μ F cm ²)	θ	%IE
ECI	Blank	3.2	100.71	50.5	00.00	00.00
	0.1	3.3	191.75	41.5	0.474	47.4
	0.3	3.7	895.83	10.8	0.887	88.7
	0.5	3.6	1278.3	0.99	0.921	92.1
SA	Blank	2.05	118	213	00.00	00.00
	0.1	2.34	351	29	0.663	66.3
	0.3	2.61	905	4.5	0.869	86.9
	0.5	3.02	1046	3.9	0.887	88.7

The decrease in C_{dl} values can be interpreted as either strengthen in inhibitor film on metal surface *i.e.* increase in thickness of the electric double layer or decrease in dielectric constant of the solution or both [8,13]. In general natural products have the lower dielectric constants and so it decreases on addition of plant extract in to corrosive solution. The %IE can also be expressed in terms of impedance parameters such as charge transfer resistance in presence of inhibitor (R_{ct}^i) and charge transfer resistance in absence of inhibitor (R_{ct}^b) have been estimated by charge transfer resistance according to eqn. 8:

$$\%IE = \frac{R_{ct}^i - R_{ct}^b}{R_{ct}^i} \times 100 \quad (8)$$

It was observed from Table-4 that the value of n increases with increasing the concentration of plant extract, which can be attributed as the formation of protective thin film at mild steel test solution interface [13].

Effect of temperature and adsorption isotherm: The adsorption of inhibitors on the metal surface depends on structure and electronic properties of inhibitor molecules, electrochemical potentials at the metal-test solution interface and the temperature of corrosive medium [13,17,18].

The adsorption isotherm, which is an important parameter for understanding the inhibition mechanism of inhibitor, was estimated by θ values, which has been derived from gravimetric analysis. A correlation between θ and inhibitor concentration in acidic medium for Langmuir's adsorption model is reported by various workers [8,19] as represented in eqn. 9:

$$\frac{C_{inh}}{\theta} = \frac{1}{K_{ads}} + C_{inh} \quad (9)$$

The values of adsorption isotherm (K_{ads}) were calculated by plotting C_{inh}/θ versus C_{inh} at 27 °C. We find a linear relationship C_{inh}/θ and C_{inh} with a correlation coefficient (R^2) of order of 0.99 as shown in Fig. 3. This suggests that the inhibition of mild steel corrosion by the adsorption of ECI and SA molecule is assumed to be monolayer with no lateral interaction between the adsorbed molecules, even on the adjacent sites [20].

The inhibitive effect of ECI and SA extracts for mild steel corrosion in 1 N HCl at different temperature were studied by gravimetric measurements at 0.1, 0.3 and 0.5 g/L concentrations of inhibitor and the obtained parameters are presented in Table-5. It is apparent from Table-5 that at a particular concentration of ECI and SA extracts, %IE decreases with rise in temperature from 27 to 67 °C. It was difficult to estimate that the inhibition is either due to physisorption or chemisorption of inhibitor molecules on the metal surface. However, we know that the physisorption is favourable at low temperature due to

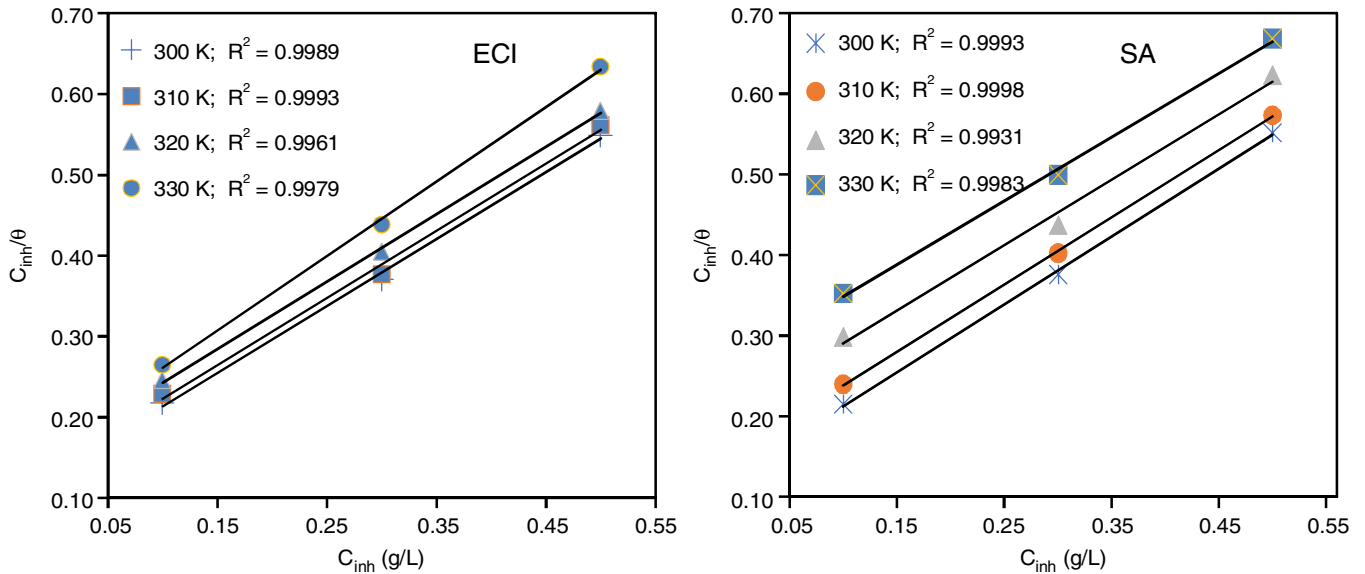


Fig. 3. Langmuir adsorption isotherm at 27 °C for the mild steel in 1 N HCl with and without various concentrations of ECI and SA extracts

Inhibitor	Temp. (K)	$-\Delta G_{ads}$	K_{ads}
ECI	300	15.08	7.64
	310	15.48	7.33
	320	15.62	6.40
	330	15.86	5.84
SA	300	15.14	7.81
	310	14.67	6.47
	320	13.91	4.77
	330	13.22	3.71

the low heat of adsorption whereas chemisorption is favourable at high temperature because of high adsorption energy [21,22]. Hence the decrease in %IE with rise in temperature can be

understood in terms of physisorption behaviour of ECI and SA extracts on the mild steel.

The values of apparent activation energy (E_a) for corrosion process were calculated in absence and presence of different concentration of inhibitors using Arrhenius equation (eqn. 10):

$$\log C_{rate} = \left(-\frac{E_a}{2.303RT} \right) + A \quad (10)$$

where E_a is the apparent activation energy, A is the frequency factor, T is the absolute temperature and R (8.314 J mol/K) is the gas constant. The values of E_a were predicted from slopes of plots of $\log C_{rate}$ against $(1/T)$, in absence and presence of different concentrations of inhibitor as presented in Fig. 4. The calculated values of E_a from the slopes are presented in Table-6, which indicated that the value of E_a increases with increase in concentration of inhibitor due to which corrosion rate decreases with increasing concentration of inhibitor.

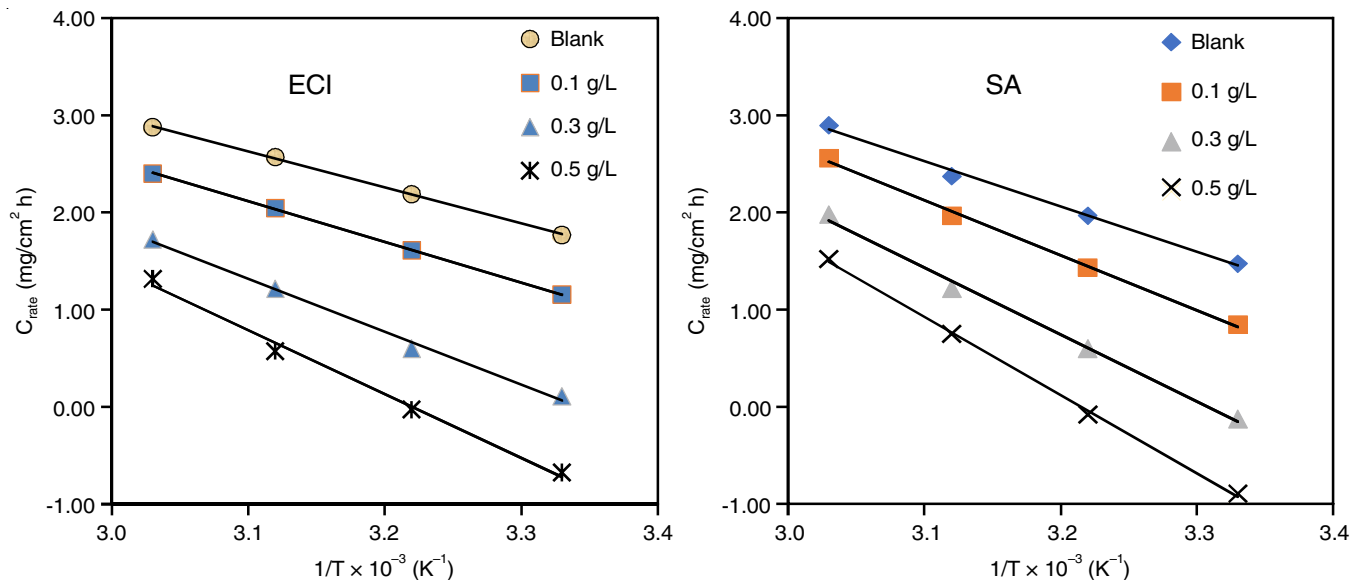


Fig. 4. Arrhenius plot for the inhibition of corrosion of mild steel in 1 N HCl without and with different concentrations of ECI and SA extracts

TABLE-6
THERMODYNAMIC ACTIVATION PARAMETERS FOR
MILD STEEL IN 1 N HCl SOLUTION OBTAINED
FROM GRAVIMETRIC MEASUREMENTS

Inhibitor	Conc. (g/L)	E_a (kJ mol ⁻¹)	ΔH^a (kJ mol ⁻¹)	$-\Delta S^a$ (J mol ⁻¹ K ⁻¹)
ECI	Blank	30.50	28.17	136.36
	0.1	34.40	32.09	128.47
	0.3	44.97	42.72	102.15
	0.5	54.06	51.86	78.22
SA	Blank	38.73	36.09	112.64
	0.1	47.12	44.49	89.96
	0.3	57.43	54.80	63.74
	0.5	66.92	64.28	38.55

The enthalpy of adsorption (ΔH^a) and the entropy of adsorption (ΔS^a) for corrosion reaction were determined through eqn. 11:

$$C_{\text{rate}} = \frac{R}{N_h} \exp\left(\frac{\Delta S^a}{R}\right) \exp\left(\frac{-\Delta H^a}{RT}\right) \quad (11)$$

here h and N are the plank's constant and Avogadro number, respectively.

The values of ΔH^a and ΔS^a were calculated from slope ($-H^a/2.303 R$) and intercept ($\log(R/N_h) + \Delta S^a/2.303 R$) on y-axis. The positive value of ΔH^a indicates that the corrosion process is endothermic in nature while a negative correlation was found between the values of ΔS^a and the concentration of inhibitor in corrosive medium (Table-6).

FT-IR studies: FT-IR study of crude extract and of the adsorbed compound on the mild steel surface in presence of inhibitor helps to identify the most probable inhibitor molecules present in ECI and SA extracts also infers the inhibition mechanism. Fig. 5a-b presents the FTIR spectra of crude methanolic extracts of ECI and SA as well as scratched protective film due to presence of 0.5 g/L of ECI and SA extracts in 1 N HCl solution at 27 °C [23].

FT-IR spectrum of methanolic extracts of ECI and SA and their corrosion reaction product on metal surface recorded in

the region 4000-400 cm⁻¹. Fig. 5a shows that a broad band appeared in the range of 3600-3000 cm⁻¹ and it can be assigned to presence of -OH vibrations [24] in crude extract. This broad band in crude extract methanolic extract results from the intermolecular hydrogen bonding [25]. This study following with GC-MS data (Table-1) suggest that the effective inhibitor molecules present in ECI extract are (-)-spathulenol, kryptogenin 2,4-dinitro phenyl hydrazone, retinoic acid and its derivatives. The band appeared at 1115 cm⁻¹ in FTIR spectrum of the methanolic extract exhibit the C-O-C stretching in retinoic acid and its derivatives. The strong peak near 1649 cm⁻¹ probably results from the COO⁻ or C=C stretching in retinoic acid and its derivatives, whereas the band near 645 cm⁻¹ is due to -C=C-H stretching.

The FTIR spectra of ECI methanolic extract of corrosion product obtained by scratching from the mild steel coupon surface showed the weaker intensity band -OH at 3361 cm⁻¹ (Fig. 5a, lower spectrum). This is probably due to formation of thin film of Fe-inhibitor complex on to the mild steel surface through -OH groups due to retinoic acid or spathulenol molecules. Disappearance of bands near 1115 and 645 cm⁻¹ also occurred due to the physisorption of inhibitor molecules onto the mild steel surface. The alteration in the strength of various bands in FT-IR spectra of corrosion product is caused by the modification in the structure of inhibitor molecules when they are present alongside metal. This modification facilitates the formation of a complex between the inhibitor and iron on the surface of mild steel in the presence of ECI extract, which complex effectively prevents corrosion from occurring on the metal surface [25].

The FT-IR spectra of the SA extract and the protective layer of the extract molecules adsorbed onto a mild steel specimen surface are shown in Fig. 5b. In Fig. 5b, extract of SA exhibit a broad band at 3389 cm⁻¹ represented O-H stretching and small band appeared at 2951 cm⁻¹ was due to the C-H stretching vibrations. The bands at 1653 cm⁻¹ and 1021 cm⁻¹ corresponded to C=C and C-O-C stretching. The spectral peaks of scratched corrosion product in presence of SA extract were shifted to 3401 and 1663 cm⁻¹; these were characteristics of C=C, C=O

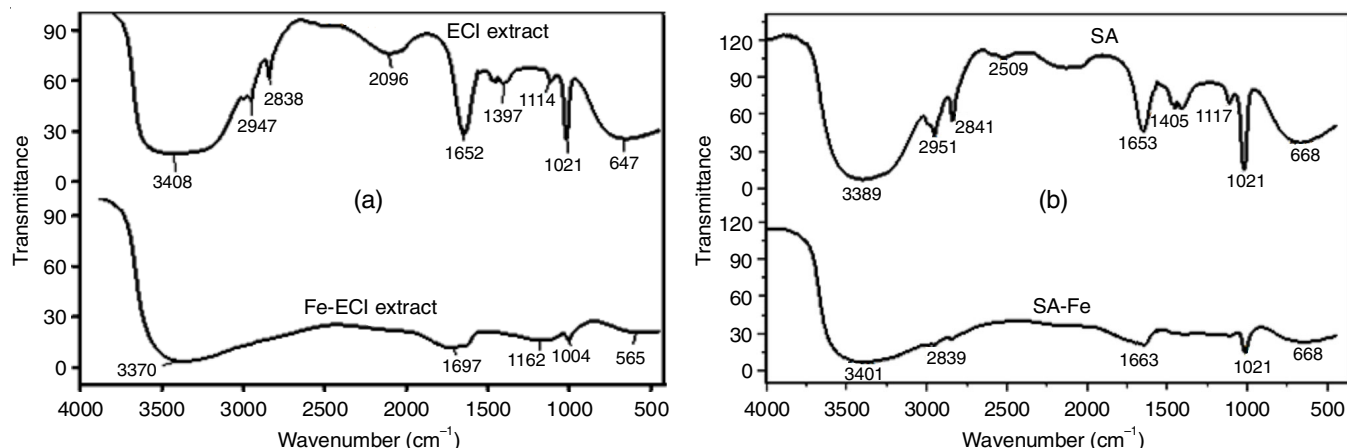


Fig. 5. (a) FT-IR spectra of pure ECI extract and protective layer developed on mild steel after immersion for 3 h in 1 N HCl containing 0.5 g/L ECI extract and (b) FT-IR spectra of pure SA extract and protective layer developed on mild steel after immersion for 3 h in 1 N HCl containing 0.5 g/L SA extract

or O-H functional group of plant extract involved in bonding with iron atom. Thus, the plant extract molecules were adsorbed onto the metal surface at the active sites.

SEM studies: The SEM images of the mild steel surface immersed in 1 N HCl for 3 h in absence and presence of 0.5 g/L of ECI and SA extracts along with SEM image for mild steel surface before immersion are presented in Fig. 6a-d. A more uniform surface of mild steel without corrosive solution 6(b). Fig. 6a,c-d present the SEM image of uninhibited and inhibited with ECI and SA extracts, respectively. Fig. 6a show highly uneven surface of mild steel due to aggressive corrosion attacks in presence of 1 N HCl solution, whereas Fig. 6c-d shows that remarkable change in the degree of corrosion [26] due to presence of ECI and SA extracts as green inhibitors.

The interaction between organic molecules present in methanolic extracts of ECI and SA can be attributed due to the reasons (i) charge-transfer-type interaction between unshared electron pairs present in oxygen or π -electrons of π -bond and empty low energy d -orbitals of Fe atom present on mild steel surface; (ii) columbic interactions between aromatic π -clouds and mild steel surface/solution interface or between protonated phytochemical molecules and adsorbed Cl^- ions at cathodic sides; and (iii) A combined effects of (i) and (ii) [27-29]. The systematic mechanism of corrosion inhibitor on mild steel by ECI and SA methanolic extracts are shown in Fig. 7.

Conclusion

Based on the results, the methanolic extracts of *Elsholtzia communis* inflorescence (ECI) and *Spilanthes acmella* (SA)

show an effective green corrosion inhibition of mild steel 1 N HCl solution. The inhibition efficiency increases with increasing the extract concentration and the inhibition efficiency reached up to 91.45% in presence of 0.5 g/L of ECI extract. Tafel polarization studies show that investigated green inhibitor acted as mixed type inhibitor but favouring more cathodic reaction suppression. The adsorption of ECI and SA extracts on mild steel surface follows the Langmuir adsorption isotherm at all the worked temperatures. Thermodynamic parameters of adsorption suggest that the interaction between mild steel surface inhibitor in physical in nature. FTIR study revealed that ECI extract probably interacted on the mild steel surface through (-)-spathulenol, retinoic acid and its derivatives, whereas SA extract may get adsorbed on the surface through its unsaturated fatty acid constituents molecule. The SEM images supported the formation of protecting layer on the mild steel surface. Temperature effects on corrosion inhibition study of ECI and SA extracts are suggested physio-sorption of inhibitor on mild steel surface with strong negative value of entropy.

ACKNOWLEDGEMENTS

The authors acknowledge the Sophisticated Instrumentation Centre for Applied Research and Training (SICART), Vallabh Vidyanagar Gujarat for helping in GC-MS study.

CONFLICT OF INTEREST

The authors declare that there is no conflict of interests regarding the publication of this article.

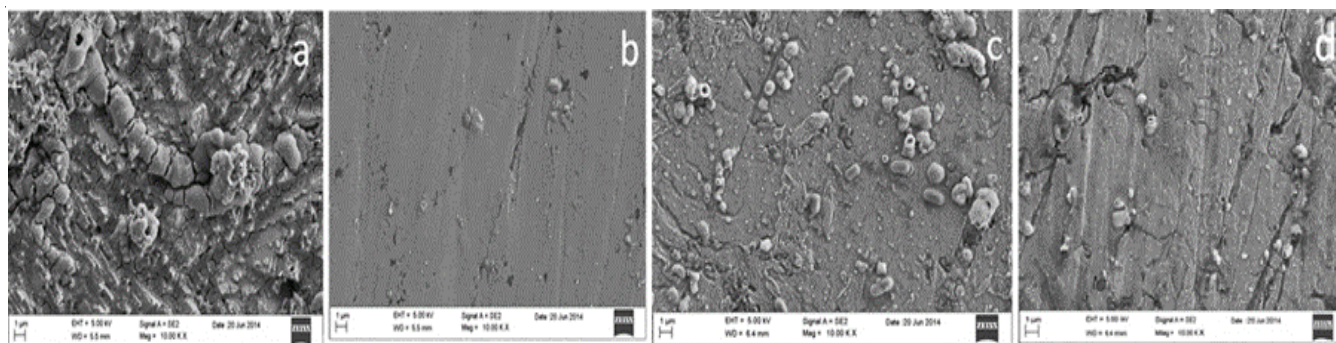


Fig. 6. SEM images of mild steel surface (a) immersed in 1 N HCl, (b) polished, (c) immersed in 1 N HCl in the presence 0.5 g/L of ECI, (d) immersed in 1 N HCl in the presence 0.5 g/L of SA

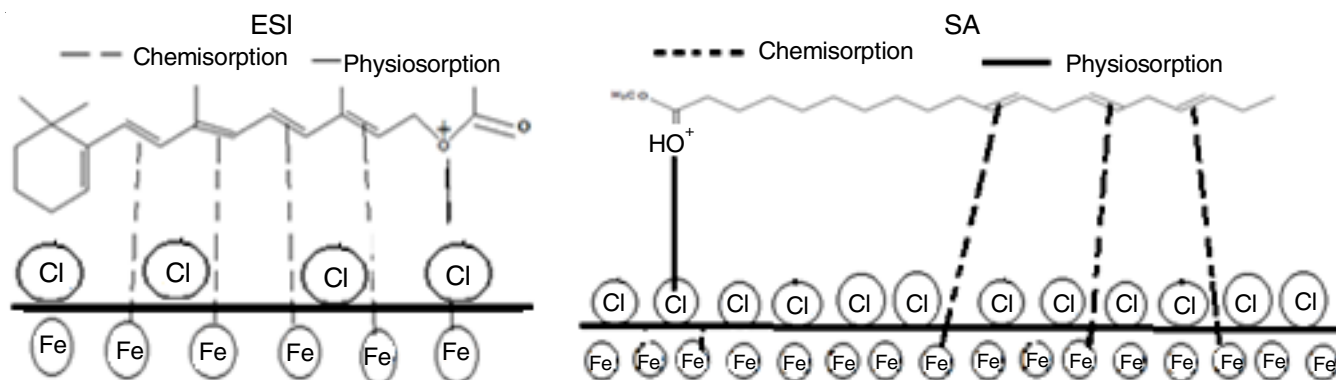


Fig. 7. Schematic diagram of corrosion inhibition reaction mechanism main constituent of ECI and SA extract on mild steel

REFERENCES

1. C.-C. Jiang, G.-Y. Xiao, X. Zhang, R.-F. Zhu and Y.-P. Lu, *New J. Chem.*, **40**, 1347 (2016); <https://doi.org/10.1039/C5NJ02245B>
2. E.E. Oguzie, Y. Li, S.G. Wang and F. Wang, *RSC Adv.*, **1**, 866 (2011); <https://doi.org/10.1039/c1ra00148e>
3. D.D.N. Singh, M.M. Singh, R.S. Chaudhary and C.V. Agarwal, *Electrochim. Acta*, **26**, 1051 (1981); [https://doi.org/10.1016/0013-4686\(81\)85076-1](https://doi.org/10.1016/0013-4686(81)85076-1)
4. D. Turcio-Ortega, T. Pandiyan, J. Cruz and E. Garcia-Ochoa, *J. Phys. Chem. C*, **111**, 9853 (2007); <https://doi.org/10.1021/jp0711038>
5. E.E. Oguzie, S.G. Wang, Y. Li and F.H. Wang, *J. Phys. Chem. C*, **113**, 8420 (2009); <https://doi.org/10.1021/jp9015257>
6. K.K. Alaneme, S.J. Olusegun and O.T. Adelowo, *Alexand. Eng. J.*, **55**, 673 (2016); <https://doi.org/10.1016/j.aej.2015.10.009>
7. A.K. Satapathy, G. Gunasekaran, S.C. Sahoo, K. Amit and P.V. Rodrigues, *Corros. Sci.*, **51**, 2848 (2009); <https://doi.org/10.1016/j.corsci.2009.08.016>
8. P. Mourya, S. Banerjee and M.M. Singh, *Corros. Sci.*, **85**, 352 (2014); <https://doi.org/10.1016/j.corsci.2014.04.036>
9. S.M.A. Hosseini, M. Salari, E. Jamalizadeh, S. Khezripor and M. Seifi, *Mater. Chem. Phys.*, **119**, 100 (2010); <https://doi.org/10.1016/j.matchemphys.2009.08.029>
10. A.S. Yaro, A.A. Khadom and H.F. Ibraheem, *Anti-Corros. Meth. Mater.*, **58**, 116 (2011); <https://doi.org/10.1108/00035591111130497>
11. V. Prachayasittikul, S. Prachayasittikul, S. Ruchirawat and V. Prachayasittikul, *Excli J.*, **12**, 291 (2013).
12. Z. Guo, Z. Liu, X. Wang, W. Liu, R. Jiang, R. Cheng and G. She, *Chem. Cent. J.*, **6**, 147 (2012); <https://doi.org/10.1186/1752-153X-6-147>
13. A.A.S. Begum, R.M.A. Vahith, V. Kotra, M.R. Shaik, A. Abdelgawad, E.M. Awwad and M. Khan, *Coatings*, **11**, 106 (2021); <https://doi.org/10.3390/coatings11010106>
14. E.E. Oguzie, C.K. Enenebeaku, C.O. Akalezi, S.C. Okoro, A.A. Ayuk and E.N. Ejike, *J. Colloid Interface Sci.*, **349**, 283 (2010); <https://doi.org/10.1016/j.jcis.2010.05.027>
15. A.O. Yuce and G. Kardas, *Corros. Sci.*, **58**, 86 (2012); <https://doi.org/10.1016/j.corsci.2012.01.013>
16. K.F. Khaled, *Mater. Chem. Phys.*, **112**, 290 (2008); <https://doi.org/10.1016/j.matchemphys.2008.05.056>
17. L. Shen, Y. Zhao, Y. Wang, R. Song, Q. Yao, S. Chen and Y. Chai, *J. Mater. Chem A*, **4**, 5044 (2016); <https://doi.org/10.1039/C6TA01604A>
18. I.M. Mejeha, M.C. Nwandu, K.B. Okema, L.A. Nnanna, F.C. Eze, M.A. Chidiebere and E.E. Oguzie, *J. Mater. Sci.*, **47**, 2559 (2012); <https://doi.org/10.1007/s10853-011-6079-2>
19. A. Khadraoui, A. Khelifa, H. Hamitouche, R. Mehdaoui, *Res. Chem. Int.*, **40**, 961 (2014); <https://doi.org/10.1007/s11164-012-1014-y>
20. A.K. Singh and M.A. Quraishi, *Corros. Sci.*, **52**, 152 (2010); <https://doi.org/10.1016/j.corsci.2009.08.050>
21. R. Karthikaiselvi and S. Subhashini, *J. Assoc. Arab Univ. Basic Appl. Sci.*, **16**, 74 (2014); <https://doi.org/10.1016/j.jaubas.2013.06.002>
22. I.B. Obot and N.O. Obi-Egbedi, *Corros. Sci.*, **52**, 198 (2010); <https://doi.org/10.1016/j.corsci.2009.09.002>
23. K.F. Khaled, *Corros. Sci.*, **52**, 2905 (2010); <https://doi.org/10.1016/j.corsci.2010.05.001>
24. A.S. Yaro, A.A. Khadom and R.K. Wael, *Alexand. Eng. J.*, **52**, 129 (2013); <https://doi.org/10.1016/j.aej.2012.11.001>
25. A.A. Rahim, E. Rocca, J. Steinmetz, M.J. Kassim, R. Adnan and M.S. Ibrahim, *Corros. Sci.*, **49**, 402 (2007); <https://doi.org/10.1016/j.corsci.2006.04.013>
26. S. Garai, S. Garai, P. Jaisankar, J.K. Singh and A. Elango, *Corros. Sci.*, **60**, 193 (2012); <https://doi.org/10.1016/j.corsci.2012.03.036>
27. D.A. López, W.H. Schreiner, S.R. de Sánchez and S.N. Simison, *Appl. Surf. Sci.*, **207**, 69 (2003); [https://doi.org/10.1016/S0169-4332\(02\)01218-7](https://doi.org/10.1016/S0169-4332(02)01218-7)
28. G. Avci, *Mater. Chem. Phys.*, **112**, 234 (2008); <https://doi.org/10.1016/j.matchemphys.2008.05.036>
29. V.V. Torres, V.A. Rayol, M. Magalhães, G.M. Viana, L.C.S. Aguiar, S.P. Machado, H. Orofino and E. D'Elia, *Corros. Sci.*, **79**, 108 (2014); <https://doi.org/10.1016/j.corsci.2013.10.032>